Modelling and Analysis of Rayleigh–Bénard convection

Xuhui Wang, Henry Jiang

December 2021

Abstract

In this project, we study an important scenario in the sub-field of Fluid Dynamics, Rayleigh-Bénard convection (also referred to as RBC), which is a buoyancy-driven flow of a fluid heated from below and cooled from above between two parallel plates. This model of thermal convection, considered as a paradigm for many non-linear and chaotic dynamics, pattern formation and fully developed turbulence, plays an fundamental and essential role in much research and application in Astrophysics, Aerodynamics and Engineering. Between the two parallel plates, the motion of flow generated by buoyancy, due to the density change caused by temperature variation, is opposed by the viscous forces in the fluid. In this project, following a step-by-step fashion, we study the mathematical model that depicts the flow motion, analyze the balance among these forces and the stability of the flow, and finally make simulation for different conditions. By stability analysis, we present that the change and behavior of the flow and the system stability in Rayleigh-Bénard convection depend on the dimensionless Rayleigh number. By numerical calculation, we present that the critical limit of the system stability, over which the flow transits from stable state to chaos, is Ra = 1707.

1 Introduction

Lord Rayleigh (1842-1919) was known as the first scientist who theoretically analyzed the RBC whose effects depend solely on a temperature gradient in 1916. In 1958, John Pearson (1930-) introduced surface tension variable to the problem, which corresponds to the original research by Henry Bénard (1874-1939). In modern, Rayleigh–Bénard convection is referred to as the fluid effects caused by temperature. RBC occurs between two parallel enclosing plates where the lower plate keeps a higher temperature while the higher plate keeps a cooler temperature. The fluid near the lower plate gets a higher temperature, and thus lower density, than the rest of the fluid. In this situation, the gravity would make the cooler and heavier fluid sink, however, the fluid motion would be opposed by the viscous force in the fluid. The balance between different forces would affect the behavior of the flow and thus the convection. In other words, the instability would occur in the fluid system. RBC is being largely adopted in many fields. Paulius *Et al.* showed the function that describes phase transition of the water vapors can be reduced to 3 when using Boussinesq's approximation scheme [1]. Stevens *Et al.* proposed that RBC could also been used in the field of the dust devil simulations [2]. The dust devils was majorly simulated using the large eddy simulation technique based on the data gathered from the field. Using the Rayleigh Benard convections, earth scientist could use the direct numerical simulation method which reduces the computation power [2]. Zhang *Et al.* used RBC to demonstrate that the roughness among the surface of a turbulent thermal convection at some instances will hinders the effectiveness of the heat transfer of the system [3]. In this project, we would

analytically present the basic model, numerically investigate the stability of the fluid motion in Rayleigh–Bénard convection and make the simulation.

In Continuum Fluid Mechanics, we treat fluid as a continuous material or a continuum, of which the local mathematical and physical properties are represented by continuous functions in terms of space and time. With this simplification, we could investigate the movement of matter on a scale larger than the distances between their fundamental particles. In other words, continuum properties make it easy to study the integrated effects of the general level physics, instead of the details appearing on the particle level physics. Countless research and applications have proved that this representation achieves high accuracy over a wide range of scenarios.

In the following sections, firstly, we would present the modelling and approximation process of the system under some basic assumptions. Secondly, we would perform the problem formation and introduce some important nondimensionless numbers for the ease of calculation and proof. Then, we would walk through the stability analysis, and finally give the simulation results of the convection.

2 Modelling

Given that Continuum Fluids Mechanics deals with the mechanical behavior of fluid modeled as a continuous mass rather than discrete particles, we could treat the fluid as many small volume element, which is the basic assumptions in Continuum Physics. Furthermore, the fundamentals of Classic Mechanics, conservation of mass, conservation of momentum and conservation of energy, are also applied in fluid dynamics. Thus, to model the fluid system by describing it as PDEs, we need to characterize a flow field by balance in mass, energy and momentum, so it is required to introduce some governing equations about conservation laws to study on the motion of flow in the same way we study on the motion of matters in Classic Mechanics. After the initial modelling, various approximations would be discussed to derive the Boussinesq's equations, a set of essential equations in the field of buoyancy-driven flow, in order to simplify the model of fluid motion in our studied scenario.

2.1 Navier–Stokes equations

Firstly, we consider the conservation of mass. Based on the continuum assumption, the net rate of mass inflow per unit volume must equal to the rate of mass increase per unit volume, which is the local rate of change of density. Figure 1 shows that the net inflow of mass along x-direction into a unit volume is $L - R$, where (x, y, z) denote the coordinate of the unit volume. We can write the conservation of mass in the form [4]:

$$\frac{\partial \rho}{\partial t} + \nabla \cdot (\rho \boldsymbol{u}) = 0 \tag{1}$$

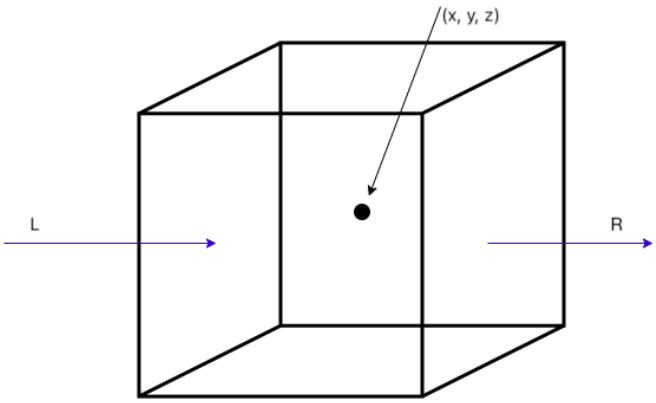

Figure 1: Net inflow of mass

where the first term of the left hand side of equation is the local rate of change of density, the second term is the divergence of mass flux, ρ is the density, $\boldsymbol{u}$ is the velocity, and t is the time variable. Applying Euler's relationship $\frac{D}{Dt} = \frac{\partial}{\partial t} + \boldsymbol{u} \cdot \nabla$ where D denotes the material derivative, we could derive this equation in an alternative form:

$$\frac{1}{\rho}\frac{D\rho}{Dt} + \nabla \cdot \boldsymbol{u} = 0. \tag{2}$$

We focus only on the case of incompressible flow that refers to a flow in which the material density is constant following the fluid motion, therefore the velocity divergence is equal to zero, which yields

$$\nabla \cdot \boldsymbol{u} = 0. \tag{3}$$

Secondly, as in the case of conservation of mass derivation, one can show that the conservation of momentum for incompressible flow, also known as the incompressible Navier-Stokes equations, is in the form [4]:

$$\rho\frac{D\boldsymbol{u}}{Dt} = -\nabla p + \rho\boldsymbol{g} + \mu\nabla^2\boldsymbol{u} \tag{4}$$

where p is the pressure of the fluid, μ is the viscosity, and g is the gravitational force.

Lastly, one can also show that the conservation of energy is in the form [4]:

$$\rho\frac{De}{Dt} = -\nabla \cdot \boldsymbol{q} - p\nabla \cdot \boldsymbol{u} + \phi \tag{5}$$

where e is the thermal energy density, $\boldsymbol{q}$ is the heat flux density, and ϕ is the rate of dissipation through viscous effects per unit volume.

So far, we have derived the necessary equations to portray the properties of an incompressible flow in motion. In the next section, some approximation methods would be introduced to simplify these governing equations.

2.2 Boussinesq's approximation

Joseph Valentin Boussinesq (1842-1929) shows that, in the case of bouyancy driven flow, the density variations could be negligible in the momentum equation (4), except in the gravity term. Additionally, The approximation also treats some other properties of fluid as constants. With this approximation, we would investigate the resulting simplification of the equations of fluid motion in our studied scenario.

In order to simplify the mass equation, we assume that the density change in the fluid is small, compared to the velocity gradients. Referencing the equation (2) yields the mass equation in another form [5]:

$$\nabla \cdot \boldsymbol{u} \approx 0. \tag{6}$$

Then, for the momentum equation (4), decomposing p and ρ into one background field in hydrostatic equilibrium and one small perturbation, the following equations could be derived:

$$p = p_0(y) + p'(x, y, t) \tag{7}$$

and

$$\rho = \rho_(y) + \rho'(x, y, t) \tag{8}$$

where $p_0(y)$ is the background field of pressure because pressure depends on y value, ρ is the background field of density, and p' and ρ' are the perturbations.

In the hydrostatic case where $\boldsymbol{u} = 0$, the conservation of momentum (4) yields

$$\nabla p_0 = \rho_0 \boldsymbol{g}. \tag{9}$$

Subtracting this from the equation (4) and dividing by ρ_0 yields [5]

$$(1 + \frac{\rho'}{\rho_0}) \frac{D\boldsymbol{u}}{Dt} = -\frac{1}{\rho_0}\nabla p' + \frac{\rho'}{\rho_0}\boldsymbol{g} + \frac{\mu}{\rho_0}\nabla^2 \boldsymbol{u} \tag{10}$$

and we specify that $\frac{\mu}{\rho_0} = \nu$ is the kinematic viscosity.

If the value of ratio of perturbation and background field, $\frac{\rho'}{\rho_0}$, is small, the left hand side of the above equation becomes $\frac{D\boldsymbol{u}}{Dt}$. This reasonable assumption gives us the equation

$$\frac{D\boldsymbol{u}}{Dt} = -\frac{1}{\rho_0}\nabla p' + \frac{\rho'}{\rho_0}\boldsymbol{g} + \nu\nabla^2 \boldsymbol{u}. \tag{11}$$

Finally, we discuss the energy equation here. When Boussinesq approximation is valid, the viscous dissipation rate ϕ could be negligable in the thermal energy [5]. However, the assumption about the small density variations is infeasible here. Considering the original mass equation (2), by multiplying it by p and rearranging the equation, we obtain

$$-p\nabla \cdot \boldsymbol{u} = \frac{p}{\rho}\frac{D\rho}{Dt}. \tag{12}$$

To simplify the energy equation, we make two important assumptions here. The first one is that the density variations are so small that they could be linearly approximated depending on the temperature T with the following form [5]

$$\rho = \rho_0(1 - \alpha(T - T_0)) \tag{13}$$

where α denotes the thermal expansion coefficient. The second one is the ideal gas assumption that the fluid molecules do not interact with each other, so using the approximation $p = \rho RT$ and $R = C_p - C_v$, where R is the gas constant, C_p is the heat energy transfer between a system and its surrounding under a constant pressure and C_v is heat energy transfer between a system and its surrounding without any change in the volume of that system, we obtain the equation [5]

$$-p\nabla \cdot \boldsymbol{u} \approx \frac{p}{\rho}(\frac{\partial \rho}{\partial T})_p \frac{DT}{Dt} = -\frac{p}{T}\frac{DT}{Dt} = -\rho(C_p - C_v)\frac{DT}{Dt}. \tag{14}$$

With the property of ideal gas $e = C_v T$, the energy equation becomes

$$\rho C_p \frac{DT}{Dt} = -\nabla \cdot \boldsymbol{q}. \tag{15}$$

Assuming Fourier's law of heat conduction

$$\boldsymbol{q} = -k\nabla T, \tag{16}$$

the energy equation could reduce to [5]

$$\frac{DT}{Dt} = \kappa \nabla^2 T \tag{17}$$

where $\kappa = \frac{k}{\rho C_p}$ denotes the thermal diffusivity.

So far, we have simplified the governing equations based on Boussinesq's approximation. In the next section, we would move on to formalize our problem.

3 Problem Formulation

Rayleigh–Bénard convection is mainly referred to as the fluid flow behavior and change caused by temperature. It occurs between two parallel enclosing plates where the lower plate keeps a higher temperature while the higher plate keeps a cooler temperature. To formalize the problem, firstly, we consider two parallel plates with infinite length and a distance h between, as in Figure 2.

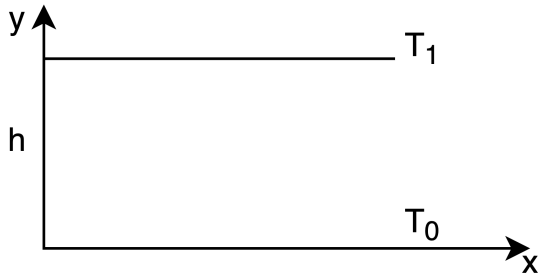

Figure 2: Problem domain

The lower plate has a higher temperature T_0 while the upper plate has a lower temperature T_1. Between the two plates, there is a fluid with density ρ, kinematic viscosity ν, thermal expansion coefficient α and thermal diffussivity κ. Ω, the problem domain where the fluid is situated, is represented by

$$\Omega : x \in \{-\infty, +\infty\}, y \in \{0, h\}. \tag{18}$$

Then we could include the problem domain in the governing equations as it follows:

$$\begin{cases} \nabla \cdot \boldsymbol{u} = \boldsymbol{0}, & x, y \in \Omega, t > 0, \\ \dfrac{D\boldsymbol{u}}{Dt} = -\dfrac{1}{\rho_0}\nabla p + \dfrac{\rho}{\rho_0}\boldsymbol{g} + \nu\nabla^2\boldsymbol{u}, & x, y \in \Omega, t > 0, \\ \dfrac{DT}{Dt} = \kappa\nabla^2 T, & x, y \in \Omega, t > 0, \\ \rho = \rho_0(1 - \alpha(T - T_0)). \end{cases} \tag{19}$$

Note that the scenario we study specifies constant temperatures at the two plates with no-slip conditions, so the boundary conditions would be given as it follows

$$\begin{cases} T(\boldsymbol{x}, t)|_{y=0} = T_0, & x \in \{-\infty, +\infty\}, t > 0, \\ T(\boldsymbol{x}, t)|_{y=h} = T_1, & x \in \{-\infty, +\infty\}, t > 0, \\ \boldsymbol{u}(\boldsymbol{x}, t)|_{y=0} = \boldsymbol{0}, & x \in \{-\infty, +\infty\}, t > 0, \\ \boldsymbol{u}(\boldsymbol{x}, t)|_{y=h} = \boldsymbol{0}, & x \in \{-\infty, +\infty\}, t > 0. \end{cases} \tag{20}$$

Additionally, the initial conditions would be given as it follows

$$\begin{cases} T(y, t)|_{t=0} = 0, & x, y \in \Omega, \\ \boldsymbol{u}(\boldsymbol{x}, t)|_{t=0} = \boldsymbol{0}, & x, y \in \Omega. \end{cases} \tag{21}$$

So far, we have finished the problem formation given the governing equations simplified by Boussinesq's approximation. To further analyze the problem and system of fluid motion, we still need to determine some important physically characteristic quantities such as Ra, the Rayleigh

number.

3.1 Non-dimensionalization

Here we introduce some dimensionless parameters by taking substitutions in these forms [6]:

$$p = U^2\rho_0\frac{\nu}{\kappa}\bar{p}, \quad \boldsymbol{u} = U\bar{\boldsymbol{u}}, \quad T = \Delta T\bar{T} + T_0, \quad \boldsymbol{x} = h\bar{\boldsymbol{x}}, \quad t = \frac{h}{U}\bar{t} \tag{22}$$

where the quantities with a bar are dimensionless, U is the velocity scale, $U^2\rho_0\frac{\nu}{\kappa}$ is the pressure scale, ΔT is the temperature scale $T_0 - T_1$, h is the length scale, and $\frac{h}{U}$ is the time scale.

Taking the coordinate transformation, we would obtain

$$\rho = \rho_0(1 - \alpha\Delta T\bar{T}), \quad \nabla = \frac{1}{h}\bar{\nabla}, \quad \frac{\partial}{\partial t} = \frac{U}{h}\frac{\partial}{\partial \bar{t}}, \quad \frac{D\boldsymbol{u}}{Dt} = \frac{U^2}{h}\frac{D\bar{\boldsymbol{u}}}{D\bar{t}}. \tag{23}$$

Inserting the above terms into the equations (19) gives [6]

$$\begin{cases} \dfrac{U^2}{h}\dfrac{D\bar{\boldsymbol{u}}}{D\bar{t}} = -\dfrac{U^2\nu}{h\kappa}\bar{\nabla}\bar{p} + \alpha\Delta T\bar{T}\bar{\boldsymbol{g}} + \dfrac{U\nu}{h^2}\bar{\nabla}^2\bar{\boldsymbol{u}}, \\ \dfrac{\Delta TU}{h}\dfrac{D\bar{T}}{D\bar{t}} = \dfrac{\Delta T\kappa}{h^2}\bar{\nabla}^2\bar{T}. \end{cases} \tag{24}$$

Then we could transform the above equations into alternate forms by rearranging terms and coefficients:

$$\begin{cases} \dfrac{D\bar{\boldsymbol{u}}}{D\bar{t}} = -\mathrm{Pr}\bar{\nabla}\bar{p} + \mathrm{Ri}\alpha\Delta T\bar{T}\boldsymbol{e}_y + \dfrac{1}{\mathrm{Re}}\bar{\nabla}^2\bar{\boldsymbol{u}}, & \bar{x} \in \{-\infty, +\infty\}, \bar{y} \in \{0, 1\}, \bar{t} > 0, \\ \dfrac{D\bar{T}}{D\bar{t}} = \dfrac{1}{\mathrm{Pe}}\bar{\nabla}^2\bar{T}, & \bar{x} \in \{-\infty, +\infty\}, \bar{y} \in \{0, 1\}, \bar{t} > 0 \end{cases} \tag{25}$$

where

$$\mathrm{Pr} = \frac{\nu}{\kappa}, \quad \mathrm{Ri} = \frac{gh}{U^2}, \quad \mathrm{Re} = \frac{Uh}{\nu}, \quad \mathrm{Pe} = \mathrm{Pr}\cdot\mathrm{Re} = \frac{Uh}{\kappa} \tag{26}$$

are Prandtl number, Richardson number, Reynolds number and Péclet number respectively, all of which are important dimensionless quantities to depict particular physical properties of matters and would be used in numerical calculations. Last but not least, to perform the stability analysis, we need to reintroduce another velocity scale here, $U_k = \dfrac{\kappa}{h}$ [6].

Then, in the same way, we could obtain the equations including the Rayleigh number in an alternate form:

$$\begin{cases} \dfrac{1}{\mathrm{Pr}}\dfrac{D\bar{\boldsymbol{u}}}{D\bar{t}} = -\bar{\nabla}\bar{p} + \mathrm{Ra}\bar{T}\boldsymbol{e}_y + \bar{\nabla}^2\bar{\boldsymbol{u}}, & \bar{x} \in \{-\infty, +\infty\}, \bar{y} \in \{0, 1\}, \bar{t} > 0, \\ \dfrac{D\bar{T}}{D\bar{t}} = \bar{\nabla}^2\bar{T}, & \bar{x} \in \{-\infty, +\infty\}, \bar{y} \in \{0, 1\}, \bar{t} > 0 \end{cases} \tag{27}$$

where Ra is the Rayleigh number and it is defined as [7]

$$\mathrm{Ra} = \frac{\alpha \Delta T g h^3}{\nu \kappa} \tag{28}$$

where g represents the gravitational acceleration. Raleigh number is an important dimensionless number associated with buoyancy-driven flow. In the scenario we study, Raleigh number could be simply considered as the ratio of the buoyancy and the viscous forces.

Then, in the same way of transformation applied to equations (20), we would obtain the boundary conditions in the scaling form:

$$\begin{cases} \bar{T}(\bar{\boldsymbol{x}}, \bar{t})|_{\bar{y}=0} = 0, & \bar{x} \in \{-\infty, +\infty\}, \bar{t} > 0, \\ \bar{T}(\bar{\boldsymbol{x}}, \bar{t})|_{\bar{y}=1} = 1, & \bar{x} \in \{-\infty, +\infty\}, \bar{t} > 0, \\ \bar{\boldsymbol{u}}(\bar{\boldsymbol{x}}, \bar{t})|_{\bar{y}=0} = \mathbf{0}, & \bar{x} \in \{-\infty, +\infty\}, \bar{t} > 0, \\ \bar{\boldsymbol{u}}(\bar{\boldsymbol{x}}, \bar{t})|_{\bar{y}=1} = \mathbf{0}, & \bar{x} \in \{-\infty, +\infty\}, \bar{t} > 0. \end{cases} \tag{29}$$

So far, leveraging the uses of dimensionless quantities and taking substitutions and coordinate transformation, we have derived the governing equations and the boundary conditions in scaling form, all of which would be used for the later calculation and analysis purposes.

Reconsidering the Rayleigh number, given the fact that it represents the ratio of the buoyancy and the viscous forces, intuitively, we would imagine that a fluid with big Rayleigh number might change its state when the buoyancy dominates the viscous forces, while it might remain its state when the viscous forces dominate the buoyancy conversely. This analysis yields a reasonable guess that the stability of buoyancy-driven flow somewhat depends on Rayleigh number. In the following sections, we will discuss what role the Rayleigh number plays in Rayleigh-Bénard convection.

4 Stability Analysis

Stability and equilibrium are important aspects in every system. The principle of the instability in buoyancy-driven flow is quite intuitive as discussed before. Consider an element of fluid near the lower plane. Simply speaking, the element is heated, so its density decreases and it goes up inside the fluid due to the buoyancy. When the element reaches near the upper plane, its density increases due to getting colder, and it would goes down inside the fluid. Nevertheless, we want to study this problem in a more theoretical way.

The common idea of stability analysis in fluid system is to introduce a small perturbation into the background field of hydrostatic equilibrium and investigate if it would decays or grows over time [8]. The flow may transit to a new state if the perturbation keeps growing. The flow may also reach unstable chaos, known as turbulence in Fluid Dynamics, if the disturbances add up further [6]. In this section, we would discuss the stability in the governing equations based on linear analysis. Then a condition would be proposed to represent the critical limit over which the fluid would transit from a stable state to an unstable state.

Because the perturbations are so small that they could be represented linearly, we introduce normal modes to simulate the perturbations in this form [5]:

$$f = \hat{f}(y)e^{ikx+\sigma t} \tag{30}$$

where f is the perturbation, $\hat{f}$ is the complex amplitude, k is the wave number in x-coordinate, and σ is the growth rate.

Looking at the equation, we would notice that the perturbation f varies depending on σ over time t. In other words, $\sigma < 0$ yields a stable solution and the perturbation will decay out, while $\sigma > 0$ yields an unstable solution and the perturbation will grow, and $\sigma = 0$ is the critical limit for the perturbation variation. That being said, the solution would be stable for any perturbation if we can show that the solution is stable for any wave number k.

4.1 Elimination of the pressure term

Note that we drop the bar symbols from the terms in the equations because we consider only the nondimensional quantities from now on. Given that we have no information about the pressure distribution in the fluid, it is necessary to eliminate the pressure term from the governing equations (27).

The vector identity yields

$$\boldsymbol{u} \cdot \nabla \boldsymbol{u} = \nabla(\frac{\boldsymbol{u} \cdot \boldsymbol{u}}{2}) + \boldsymbol{\omega} \times \boldsymbol{u} \tag{31}$$

where $\boldsymbol{\omega}$ denotes the vorticity, which could be inserted into equations (27), yielding a new form of the governing equations:

$$\frac{1}{\mathrm{Pr}}(\frac{\partial \boldsymbol{u}}{\partial t} + \nabla(\frac{\boldsymbol{u} \cdot \boldsymbol{u}}{2}) + \boldsymbol{\omega} \times \boldsymbol{u}) = -\nabla p + \mathrm{Ra}T\boldsymbol{e}_y + \nabla^2 \boldsymbol{u}. \tag{32}$$

We take the curl of the above equation and use the fact that the curl of gradient is zero, obtaining:

$$\frac{1}{\mathrm{Pr}}(\frac{\partial}{\partial t}(\nabla \times \boldsymbol{u}) + \nabla \times \boldsymbol{\omega} \times \boldsymbol{u}) = \nabla \times \mathrm{Ra}T\boldsymbol{e}_y + \nabla^2(\nabla \times \boldsymbol{u}). \tag{33}$$

Note that the vorticity $\boldsymbol{\omega} = \nabla \times \boldsymbol{u}$. Applying

$$\nabla \times \boldsymbol{\omega} \times \boldsymbol{u} = \nabla \times \mathrm{Ra}T\boldsymbol{e}_y \times \nabla^2 \omega \tag{34}$$

generates

$$\frac{1}{\mathrm{Pr}}(\frac{\partial \omega}{\partial t} + \boldsymbol{u} \cdot \nabla \boldsymbol{\omega} - \boldsymbol{\omega} \cdot \nabla \boldsymbol{u}) = \nabla \times \mathrm{Ra}T\boldsymbol{e}_y + \nabla^2 \omega. \tag{35}$$

So far we have eliminated the pressure term from the governing equations. As we consider only the 2D flow case, which could be easily generalized to 3D domain, $T = T(x, y, t)$ and $\boldsymbol{u} = u_x(x, y, t)\boldsymbol{e}_x + u_y(x, y, t)\boldsymbol{e}_y$ yield

$$\begin{cases} \boldsymbol{\omega} = (\dfrac{\partial u_y}{\partial x} - \dfrac{\partial u_x}{\partial y})\boldsymbol{e}_z = \omega \boldsymbol{e}_z, \\ \boldsymbol{\omega} \cdot \nabla \boldsymbol{u} = 0, \\ \nabla \times T\boldsymbol{e}_y = \dfrac{\partial T}{\partial x}\boldsymbol{e}_z. \end{cases} \tag{36}$$

By rearranging and substituting the terms, finally we obtain the governing equations in the following form:

$$\begin{cases} \dfrac{1}{\mathrm{Pr}}(\dfrac{\partial \omega}{\partial t} + \boldsymbol{u} \cdot \nabla \boldsymbol{\omega}) = \mathrm{Ra}\dfrac{\partial T}{\partial x} + \nabla^2, \\ \dfrac{\partial T}{\partial t}\boldsymbol{u} \cdot \nabla T = \nabla^2 T. \end{cases} \tag{37}$$

4.2 Linearization

To introduce disturbances from the background state to the equations, we denote $\tilde{\boldsymbol{u}}', T'$ and ω' as perturbations here, and $\tilde{\boldsymbol{u}}' = \boldsymbol{0}, \tilde{T} = \tilde{T}(y)$ and $\tilde{\omega} = 0$. The background temperature field, $\tilde{T}(y)$, is found from the equations (37) by setting $\boldsymbol{u} = \boldsymbol{0}$ and $\omega = 0$, thus yielding

$$\nabla^2 \tilde{T}(y) = \frac{\partial^2 \tilde{T}}{\partial y^2} = 0. \tag{38}$$

Applying the boundary conditions $T(0) = 0, T(1) = 1$ yielding $\tilde{T}(y) = y$, substituting $T = \tilde{T}(y) + T', \boldsymbol{u} = \boldsymbol{u}'$ and $\omega = \omega'$ into the equations (37) and neglecting the higher order terms give the equations for the disturbances in the following form:

$$\begin{cases} \dfrac{1}{\mathrm{Pr}}\dfrac{\partial \omega}{\partial t} = \mathrm{Ra}\dfrac{\partial T'}{\partial x} + \nabla^2 \omega', \\ \dfrac{\partial T'}{\partial t} + u_y' = \nabla^2 T'. \end{cases} \tag{39}$$

The three unknowns, u_y', ω' and T', in the above equations could be reduced by introducing the stream functions, $\psi_x' = \frac{\partial \psi'}{\partial y}$, $\psi_y' = -\frac{\partial \psi'}{\partial x}$ and $\omega = -\nabla^2 \psi$ and substituting into the above equations, yielding the resulting equations in the following form:

$$\begin{cases} \dfrac{1}{\mathrm{Pr}}\dfrac{\partial}{\partial t}\nabla^2 \psi' = -\mathrm{Ra}\dfrac{\partial T'}{\partial x} + \nabla^2(\nabla^2 \psi'), \\ \dfrac{\partial T'}{\partial t} - \dfrac{\partial \psi'}{\partial x} = \nabla^2 T', \end{cases} \tag{40}$$

with the boundary conditions

$$\begin{cases} u_x(0) = u_y(0) = \dfrac{\partial u_y}{\partial y}(0) = 0 \Rightarrow \dfrac{\partial \psi}{\partial y}(0) = 0, \\ u_x(1) = u_y(1) = \dfrac{\partial u_y}{\partial y}(1) = 0 \Rightarrow \dfrac{\partial \psi}{\partial y}(1) = 0, \\ T(0) = 0, T(1) = 1, T' = T - \tilde{T} \Rightarrow T'(0) = T'(1) = 0. \end{cases} \tag{41}$$

4.3 Eigenvalue problem

The governing equations in the above form are linear and do not depend on x and t, then the normal mode guess could be introduced to represent

$$\begin{cases} \psi' = \hat{\psi}(y)e^{ikx+\sigma t}, \\ T' = \hat{T}(y)e^{ikx+\sigma t} \end{cases} \tag{42}$$

where $\hat{\psi}(y)$ is the complex amplitude of ψ' and $\hat{T}$ is complex amplitude of T'. By substituting these into the above equations, we obtain the governing equations in this form:

$$\begin{cases} \frac{1}{\mathrm{Pr}}\sigma(\frac{\mathrm{d}^2}{\mathrm{d}y^2} - k^2)\hat{\psi} = -\mathrm{Ra}ik\hat{T} + (\frac{\mathrm{d}^2}{\mathrm{d}y^2} - k^2)^2\hat{\psi}, \\ \sigma\hat{T} - ik\hat{\psi} = (\frac{\mathrm{d}^2}{\mathrm{d}y^2} - k^2)\hat{T}. \end{cases} \tag{43}$$

Recall that $\sigma = 0$ is the critical limit of the stable solution of the system as in the case where $\sigma = 0$ in the governing equations

$$\begin{cases} 0 = -\mathrm{Ra}ik\hat{T} + (\frac{\mathrm{d}^2}{\mathrm{d}y^2} - k^2)^2\hat{\psi}, \\ -ik\hat{\psi} = (\frac{\mathrm{d}^2}{\mathrm{d}y^2} - k^2)\hat{T}, \end{cases} \tag{44}$$

therefore, simplified by connecting these two equations using T, the governing equations become

$$k^2\hat{\psi} = \frac{1}{\mathrm{Ra}}(\frac{\mathrm{d}^2}{\mathrm{d}y^2} - k^2)^3\hat{\psi}. \tag{45}$$

Finally, a linear ODE is derived and this is an eigenvalue problem with the eigenvalue about Ra and the eigenfunction $\hat{\psi}$. Since that the equation represents the relationship between the wave number k, Rayleigh number and stream function at the critical limit of the stable system, then the eigenvalue, given k, would generate the Rayleigh number that yields a stable solution of this equation.

To solve the equation, we still have to specify the boundary conditions which, upon similar substitution and transformation discussed above, could be represented as

$$\begin{cases} \hat{T}(0) = \hat{T}(1) = 0, \\ \frac{\mathrm{d}\hat{\psi}}{\mathrm{d}y}(0) = \frac{\mathrm{d}\hat{\psi}}{\mathrm{d}y}(1) = 0, \\ (\frac{\mathrm{d}^2}{\mathrm{d}y^2} - k^2)^2\hat{\psi}(0) = (\frac{\mathrm{d}^2}{\mathrm{d}y^2} - k^2)^2\hat{\psi}(1) = 0. \end{cases} \tag{46}$$

Given that the equation (45) is ODE with constant coefficients, a guess, $\hat{\psi}(y) = e^{\alpha y}$ where α is the grow rate, could be introduced to generate a new equation:

$$k^2 + \frac{1}{\mathrm{Ra}}(\alpha^2 - k^2)^3 = 0. \tag{47}$$

The equation has 6 roots:

$$\begin{cases} i\alpha_0 = \pm ik(-1 + (\frac{\mathrm{Ra}}{k^4})^{\frac{1}{3}})^{\frac{1}{2}}, \\ \alpha_1 = \pm k(1 + (\frac{\mathrm{Ra}}{k^4})^{\frac{1}{3}}(\frac{1}{2} + i\frac{\sqrt{3}}{2}))^{\frac{1}{2}}, \\ \alpha_2 = \pm k(1 + (\frac{\mathrm{Ra}}{k^4})^{\frac{1}{3}}(\frac{1}{2} - i\frac{\sqrt{3}}{2}))^{\frac{1}{2}}. \end{cases} \tag{48}$$

Given that the perturbation could be assumed linearly as discussed before, the disturbance could be represented by a superpositions of perturbations. In the above case, the solution of the equation could be expressed as

$$\hat{\psi}(y) = Ae^{\alpha_0 y} + Be^{-\alpha_0 y} + Ce^{\alpha_1 y} + De^{-\alpha_1 y} + Ee^{\alpha_2 y} + Fe^{-\alpha_2 y} \tag{49}$$

where A, B, C, D, E and F are all constant.

Applying the boundary conditions into the solution, we obtain a system of equations in matrix form, $\boldsymbol{Ax} = \boldsymbol{0}$, where $\boldsymbol{A} =$

$$\begin{bmatrix} 1 & 1 & 1 & 1 & 1 & 1 \\ e^{\alpha_0} & e^{-\alpha_0} & e^{\alpha_1} & e^{-\alpha_1} & e^{\alpha_2} & e^{-\alpha_2} \\ \alpha_0 & -\alpha_0 & \alpha_1 & -\alpha_1 & \alpha_2 & -\alpha_2 \\ \alpha_0 e^{\alpha_0} & -\alpha_0 e^{-\alpha_0} & \alpha_1 e^{\alpha_1} & -\alpha_1 e^{-\alpha_1} & \alpha_2 e^{\alpha_2} & -\alpha_2 e^{-\alpha_2} \\ (\alpha_0^2 - k^2)^2 & (\alpha_0^2 - k^2)^2 & (\alpha_1^2 - k^2)^2 & (\alpha_1^2 - k^2)^2 & (\alpha_2^2 - k^2)^2 & (\alpha_2^2 - k^2)^2 \\ (\alpha_0^2 - k^2)^2 e^{\alpha_0} & (\alpha_0^2 - k^2)^2 e^{-\alpha_0} & (\alpha_1^2 - k^2)^2 e^{\alpha_1} & (\alpha_1^2 - k^2)^2 e^{-\alpha_1} & (\alpha_2^2 - k^2)^2 e^{\alpha_2} & (\alpha_2^2 - k^2)^2 e^{-\alpha_2} \end{bmatrix} \tag{50}$$

and $\boldsymbol{x} = [A, B, C, D, E, F]^T$.

Recall that the homogeneous equations has non-trivial solutions when the determinant of the coefficient matrix is 0, which means that the governing equation at stable limit discussed previously has at least one solution when $\det(\boldsymbol{A}) = 0$. Finally we have a method of solving for the critical limit of the stable system.

Looking at the roots (48) of the equation and the value of the matrix $\boldsymbol{A}$, we would notice that, given a wave number k value, we could numerically compute the exact Rayleigh number that yields $\det(\boldsymbol{A}(\mathrm{Ra}))|_k = 0$ using some iterative calculation method such as Newton's method. The code of solving this problem using Matlab is included in the appendix. In Figure 3, we can observe that the greatest Rayleigh number that is able to lead a stable system is approximately between [1707, 1708]. The range of wave number k is set to [1, 10], and will increase 0.01 for each computation.

So far, we have presented the stability analysis of the system by introducing normal modes, linearization, streamfunction and solving eigenvalue problem. To verify the analysis result, we would make some simulation about the flow behavior in the system.

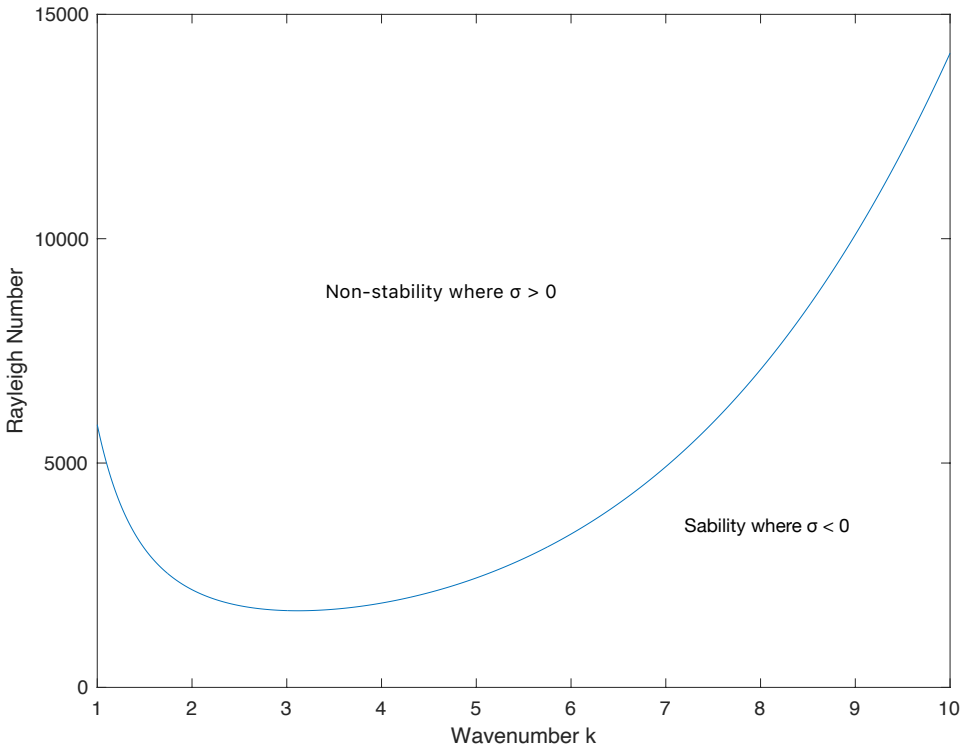

Figure 3: Stability field

5 Simulation

In this section, we would visually illustrate the Rayleigh-Bénard convection on unstable condition and stable condition respectively. All the parameters involved are upon scaling. The simulation is performed using Python package Dedalus. The code and an animation demo are also included in the appendix.

To form the numerical simulations, we start with the governing equations (25) and the corresponding continuity equation. We replace the infinite region with a finite one for the ease of numerical computation:

$$\Omega = \{(x, y); x \in (0, L_x), y \in (0, 1)\} \tag{51}$$

where L_x is the dimension of the problem domain in the x-direction.

Substituting the terms into the original equations, we have a new form of the governing equations:

$$\begin{cases} \dfrac{D\boldsymbol{u}}{Dt} = -\mathrm{Pr}\nabla p + \mathrm{Ra}\alpha\Delta T T\boldsymbol{e}_y + \dfrac{1}{\mathrm{Re}}\nabla^2\boldsymbol{u}, & \boldsymbol{x}\in\Omega, t>0, \\ \dfrac{DT}{Dt} = \dfrac{1}{\mathrm{Pe}}\nabla^2 t, & \boldsymbol{x}\in\Omega, t>0, \\ \nabla\cdot\boldsymbol{u} = 0, & \boldsymbol{x}\in\Omega, t>0. \end{cases} \tag{52}$$

The boundary conditions in x-direction is also replaced by periodicity, yielding

$$\begin{cases} T(\boldsymbol{x},t)|_{y=0} = T_0, & x\in[0,L_x], t>0, \\ T(\boldsymbol{x},t)|_{y=h} = T_1, & x\in[0,L_x], t>0, \\ \boldsymbol{u}(\boldsymbol{x},t)|_{y=0} = \boldsymbol{u}(\boldsymbol{x},t)|_{y=h} = \boldsymbol{0}, & x\in[0,L_x], t>0, \\ \boldsymbol{u}(\boldsymbol{x},t) = \boldsymbol{u}(\boldsymbol{x}+L_x\boldsymbol{e}_x,t), & y\in[0,1], t>0, \end{cases} \tag{53}$$

Additionally, the initial conditions are represented by a constant temperature and velocity field with the random noise $\boldsymbol{u}_0(\boldsymbol{x})$:

$$\begin{cases} T(y,0)|_{t=0} = T_0, & \boldsymbol{x}\in\Omega, \\ \boldsymbol{u}(\boldsymbol{x},0)|_{t=0} = \boldsymbol{u}_0(\boldsymbol{x}), & \boldsymbol{x}\in\Omega. \end{cases} \tag{54}$$

Firstly, we would present the case of unstable flow where Ra = 100,000. The value of Rayleigh number is considerably higher than the critical limit of stability, but it is a very common value for engineering purposes.

From the Figure 4 to 9, where the red region represents the hotter flow and the blue represents the colder flow, we could clearly observe how the unstable flow changes and how the convection rolls shape and deform. Figure 4 shows that the introduction of the perturbations leads to the beginning of the unstable flow. Figure 5 shows the time point since which the convection rolls start to shape and the temperature changes non-regularly over the whole fluid field. From Figure 6 to Figure 8, the higher ratio of buoyancy and viscous forces results in the wave-shaped temperature distribution and bigger convection rolls. Finally, from Figure 9, we could see that the the flow has reached a chaotic state. Limited by the due time, we are not able to perform finer and more accurate simulation of the convection, but it could be expected that the flow motion will keep chaotic and thus generate more unstable and complex turbulence over time.

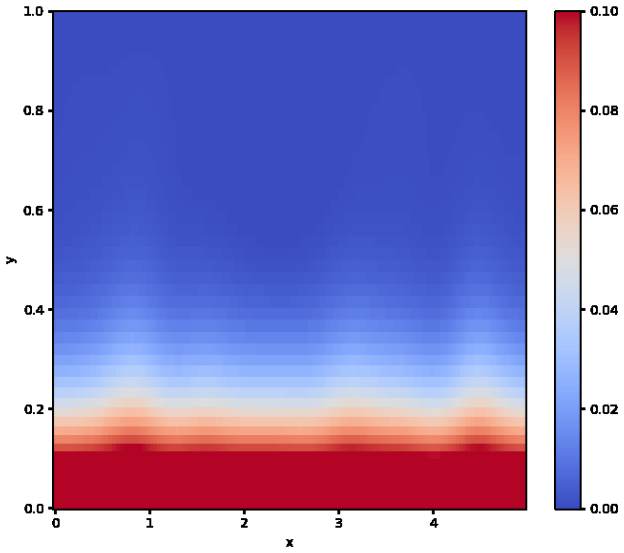

Figure 4: Raleigh number = 100,000 and $t = 1$

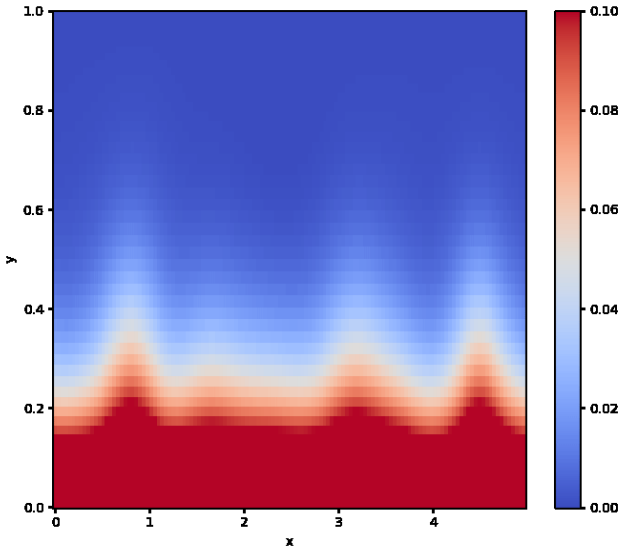

Figure 5: Raleigh number = 100,000 and $t = 2$

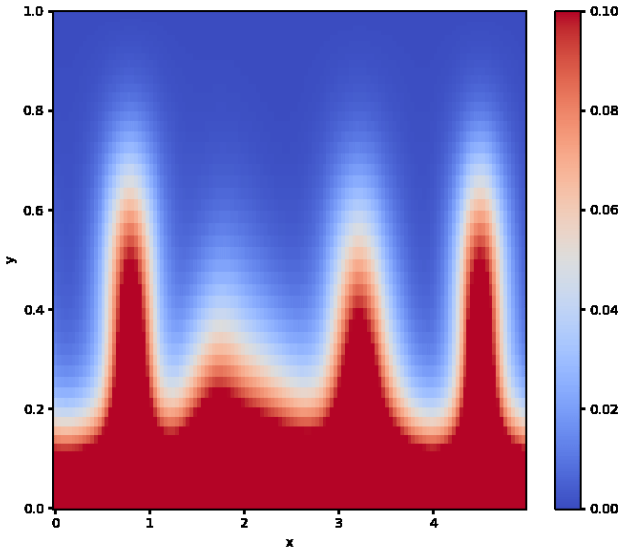

Figure 6: Raleigh number = 100,000 and $t = 3$

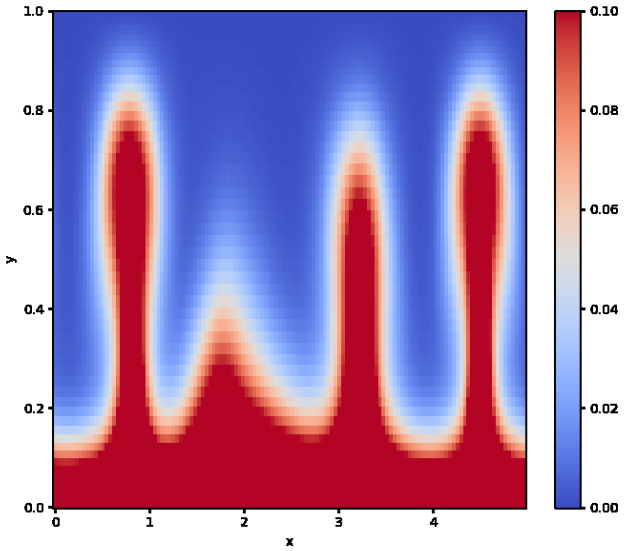

Figure 7: Raleigh number = 100,000 and $t = 4$

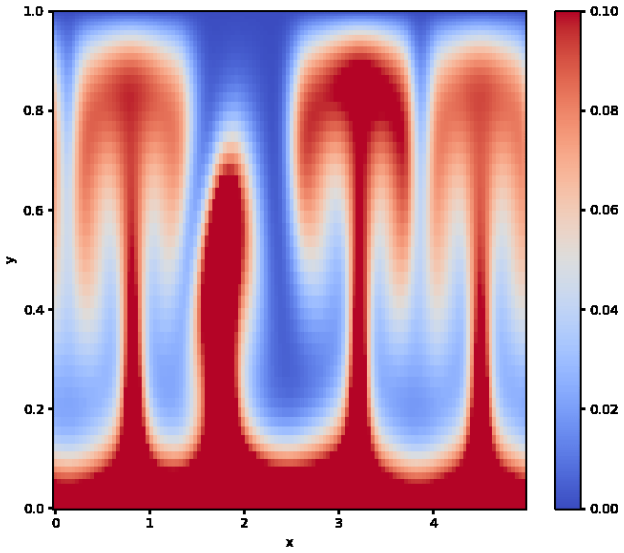

Figure 8: Raleigh number = 100,000 and $t = 5$

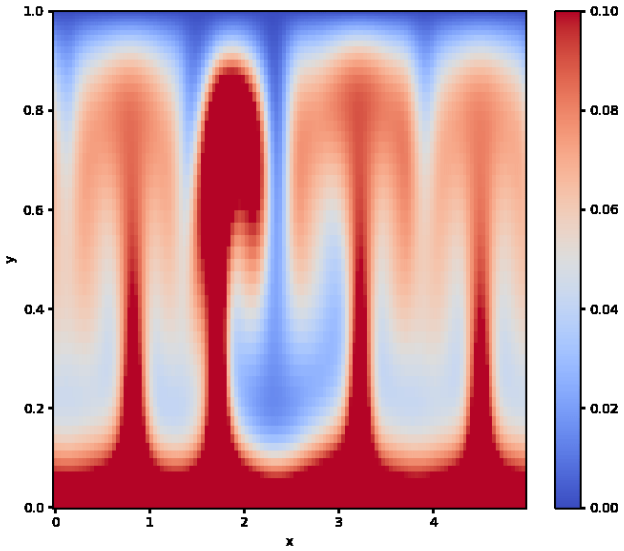

Figure 9: Raleigh number = 100,000 and $t = 6$

Then, we would present the case of stable flow where Ra < 1707. Because our program always crashes when the Rayleigh number is small and we do not have enough time to write the code for the case of pure conduction without convection, we provide other's simulation figure [9]. As the Figure 10 shows, when the Rayleigh number is small, we would expect a stable flow as discussed

earlier. The temperature is linearly distributed vertically over the y-direction. In other words, the system remains stratified in temperature over time.

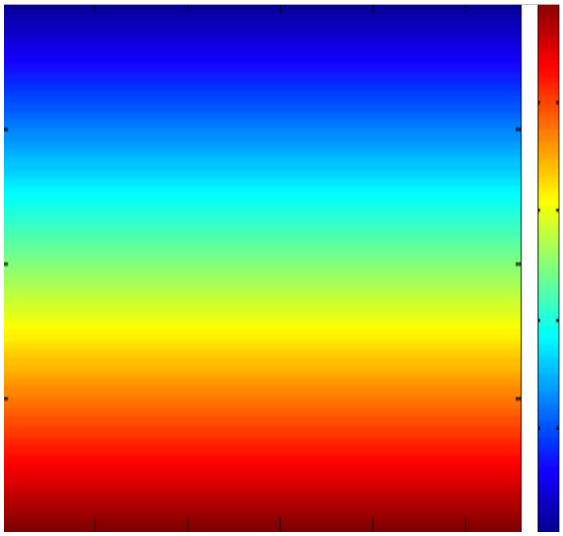

Figure 10: Small Raleigh number

6 Assessment

Based on Navier-Stokes' equations and boussinesq's approximation, the governing equations accurately model the flow motion in Rayleigh-Bénard convection with almost all of the physical properties of fluid. Besides, the form of the governing equations makes it easier to compute many physical quantities including velocity, pressure and so on. The computation and tests about these quantities are very important in simulation of Science and Engineering application. The results of stability analysis upon the model are also verified by simulation. So, the strengths and value of the model is appreciable.

However, given that there are many unknowns and non-linear terms in the model, people have to make different assumptions and optimizations to apply the model in different scenarios to ease the equations, in order to numerically compute the solutions for different problems. Though we have great interest in fluid simulation, we do not even dare to think about solving Navier-Stokes' equations. We just hope that there will be solutions in the future.

7 Conclusion

In this project, we systematically study the modelling, stability analysis of Rayleigh-Bénard convection and make the simulation. The numerical analysis of stability is also performed. We conclude that the change and behavior of flow in Rayleigh-Bénard convection depend on the dimensionless Rayleigh number. Ra = 1708 is the critical limit of the system stability. A smaller Rayleigh number than that value leads to a stable flow, while a larger Rayleigh number than that value leads to an unstable flow, and thus generating turbulence.

References

[1] O. Pauluis and O. Schumacher, "Idealized moist rayleigh-bénard convection with piecewise linear equation of state," *Commun. Math. Sci.*, vol. 8, pp. 295–319, Mar. 2010. DOI: 10.4310/CMS.2010.v8.n1.a15.

[2] R. J. A. M. STEVENS, R. VERZICCO, and D. LOHSE, "Radial boundary layer structure and nusselt number in rayleigh–bénard convection," *Journal of Fluid Mechanics*, vol. 643, pp. 495–507, 2010. DOI: 10.1017/S0022112009992461.

[3] Y.-Z. Zhang, C. Sun, Y. Bao, and Q. Zhou, "How surface roughness reduces heat transport for small roughness heights in turbulent rayleigh–bénard convection," *Journal of Fluid Mechanics*, vol. 836, R2, 2018. DOI: 10.1017/jfm.2017.786.

[4] P. K. Kundu, I. M. Cohen, and D. R. Dowling, *Fluid mechanics*, 2016.

[5] I. Mutabazi, J. Wesfreid, and E. Guyon, "The context of bénard scientific work and nonlinear science," in Jun. 2010, vol. 207, pp. 3–8, ISBN: 978-0-387-40098-3. DOI: 10.1007/978-0-387-25111-0_1.

[6] G. J. Maja Sandberg Niclas Berg, *Rayleigh–bénard convection*.

[7] MIT, *9 fluid dynamics and rayleigh-bénard convection*. [Online]. Available: https://dspace.mit.edu/bitstream/handle/1721.1/84612/12-006j-fall-2006/contents/lecture-notes/lecnotes9.pdf.

[8] G. A.V., *Rayleigh-benard convection: Structures and dynamics*, 1997.

[9] *Rayleigh-benard instability*. [Online]. Available: http://hmf.enseeiht.fr/travaux/CD0001/travaux/optmfn/hi/01pa/hyb72/rb/rb.htm.